DOI 10.1007/s10717-025-00774-6
Glass and Ceramics, Vol. 82, Nos. 5 – 6, September, 2025 (Russian Original, Nos. 5 – 6, May – June, 2025)

UDC 54-161.6:544.2

ELECTRIC POLARIZATION AND MAGNETIC PROPERTIES OF ZINC–TELLURITE GLASSES ACTIVATED BY NANOPARTICLES OF MAGNETITE AND BARIUM TITANATE

M. V. Shestakov[1] and I. I. Makoed[2]

Translated from *Steklo i Keramika*, No. 6, pp. 3 – 10, June, 2025.

Original article submitted January 25, 2025.

Samples of zinc–tellurite glasses, activated by magnetite and barium titanate nanoparticles, were synthesized by the melt quenching technique. Functional properties of the glasses were experimentally investigated by the methods of XRD analysis, optical and polarization spectroscopy, and SQUID magnetometry. The XRD data confirmed the amorphous structure of the glasses. The bandgap values of the samples were obtained based on the optical spectroscopy data. The study of electric and magnetic field dependencies of electric polarization and specific magnetization established the evolutionary development of the shape of electric and magnetic hysteresis loops depending on the composition of glasses due to the interaction of charged γ-Fe_2O_3 clusters and barium titanate nanoparticles.

Keywords: glass, tellurium oxide, zinc oxide, magnetite, barium titanate, polarization, magnetism.

INTRODUCTION

Zinc–tellurite glasses continue to attract the research attention due to their pronounced nonlinearity of optical properties and high glass-forming capacity when quenching the melt from 800 – 950 to 100 – 300°C [1 – 3]. Nominally pure tellurite glasses consist mainly of TeO_4 structural elements and exhibit a weak glass-forming ability [4]. To overcome this disadvantage, zinc–tellurite glasses are synthesized with the addition of a modifier in the form of zinc oxide. The study [5] of $(1 – x)TeO_{2–x}Fe_3O_4$ glass compositions with x varying in the 0.1 – 0.4 range found that an increase in the ZnO content in the specified limits led to a decrease in the glass transition temperature from 385 to 347°C. During synthesis, the destruction of TeO_4 structural elements and the formation of TeO_3 and TeO_{3+1} polyhedra were found to occur simultaneously. The authors [6] reported that the modification of zinc–tellurite glasses with alumina leads to a significant increase in the glass transition temperature, a decrease in the glass density, and the destruction of TeO_4 structural elements with the formation of Te–O–Al bridge bonds.

A number of publications present data on the modification of the absorption spectra of zinc–tellurite glasses by adding nickel [7], cobalt [8], or chromium [9] ions to the composition. The glasses of the TeO_2–ZnO–La_2O_3–Na_2O composition modified with erbium oxide were used to manufacture light waveguides and generate light pulses with an energy of 10 nJ and a duration of less than 100 fsec under diode pumping at 975 nm [10]. Other authors [11] studied $[ZnO]_x[(TeO_2)_{0.7}(PbO)_{0.3}]_{1–x}$ glasses and reported an increase in their bandgap from 3.41 to 3.94 eV and an increase in their refractive index from 2.50 to 2.58 when increasing the zinc oxide concentration from 0 to 25 mol.%. Along with the changes in optical properties, a number of works published data on the changes in the dielectric susceptibility and the occurrence of a ferromagnetic response upon addition of $BiFeO_3$ [12] and Fe_3O_4 [13] to the composition of zinc–tellurite glasses. According to [14], activation of glasses with minor amounts of Fe_3O_4 also shifts the optical absorption edge to the visible spectrum and a change in the polarization properties of the synthesized materials.

In this work, we aim to synthesize zinc–tellurite $(20ZnO – (80–x–y)TeO_{2–x}Fe_3O_{4–y}BaTiO_3$, where $x, y = 0; 1$) glasses activated with 1 mol.% $BaTiO_3$ and 1 mol.% Fe_3O_4, as well as to study the physical properties of the obtained materials.

[1] Moscow Institute of Physics and Technology, Dolgoprudny, Russia (e-mail: shestakov.mv@mipt.ru).
[2] Brest State University named after A. S. Pushkin, Brest, Belarus (e-mail: igmak2010@yandex.by).

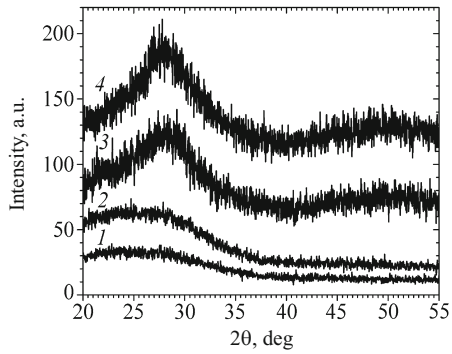

Fig. 1. XRD patterns of zinc–tellurite glasses of nominally pure composition ($20ZnO - 80TeO_2$) (*1*), those activated by magnetite ($20ZnO - 79TeO_2 - 1Fe_3O_4$) (*2*) and barium titanate ($20ZnO - 79TeO_2 - 1BaTiO_3$) (*3*) nanoparticles, and simultaneously containing magnetite and barium titanate ($20ZnO - 78TeO_2 - 1Fe_3O_4 - 1BaTiO_3$) (*4*).

EXPERIMENTAL

Zinc–tellurite glasses, both nominally pure and activated with nanosized magnetite- and barium-titanate particles, were synthesized by the melt quenching technique [15, 16]. The source reagents were TeO_2 (puratronic grade, Alfa Aesar), ZnO (puratronic grade, Alfa Aesar), Fe_3O_4 nanopowder (50 – 100 nm, 97%, Sigma-Aldrich), and $BaTiO_3$ (< 44 μm, 99.95%, Alfa Aesar). The chemical compositions of the glass batch can be described as follows: $20ZnO - 80TeO_2$, $20ZnO - 79TeO_2 - 1Fe_3O_4$, $20ZnO - 79TeO_2 - 1BaTiO_3$, $20ZnO - 78TeO_2 - 1Fe_3O_4 - 1BaTiO_3$. Here, the digital multipliers indicate the content of the corresponding components in mole percentage. The batches with the specified compositions were thoroughly ground in a mortar and then placed in a corundum crucible. The crucible was covered with a lid to prevent evaporation of the melt components and then placed in a vertical tube furnace preheated to a temperature of 850°C. After exposure at the specified temperature for 20 min, the crucible was removed from the furnace, and the melt was poured into an aluminum mold at room temperature. The obtained glasses were cut to obtain samples in the form of ($5 \times 5 \times 3$ mm^3) square plates, which were polished and used to carry out optical measurements.

The amorphous state of the glasses was confirmed by XRD data recorded by a PANAlytical X'Pert Pro diffractometer with CuKá radiation (λ = 1.5418 Å). The optical density of the glasses was studied using a Bruker Vertex 80V Fourier Transform Fourier spectrometer equipped with GaP and Si detectors. Raman spectra were recorded using a spectral analytical complex based on a Nanofinder scanning confocal microscope (JV LOTIS TII, Republic of Belarus) using a diffraction grating of 600 lines/mm. The spectra were excited by a laser with a wavelength of 473 nm and a power of 800 μW; the signal was collected by an optical objective with a magnification of × 100 for 30 sec. Magnetometry measurements were performed using a Quantum Design MPMSXL-5 SQUID magnetometer at room (300 K) and low (5 K) temperatures. The electric field dependencies of polarization of the samples were measured in the dynamic hysteresis mode with triangular excitation pulses and internal leakage compensation by a TF2000E analyzer (aixACCT) at room temperature. The frequency and amplitude of the electromagnetic pulse were 1 kHz and 400 V, respectively. The measurements were carried out on a flat capacitor-type geometry with platinum contacts with a diameter of 1130 μm.

RESULTS AND DISCUSSION

Figure 1 presents the XRD patterns of the synthesized glasses. The angular dependencies obtained have the form of broad intense reflections and a broad halo in the ranges from 20 to 35° (all glasses) and from 40 to 55° ($20ZnO - 80TeO_2$ and $20ZnO - 79TeO_2 - 1Fe_3O_4$ glasses), respectively, characteristic of an amorphous state.

The Raman spectra of nominally pure and activated glasses in the wavenumber range from 200 to 900 cm^{-1} (Fig. 2*a*) show broad bands characteristic of zinc–tellurite glasses. The signals with a Stokes shift of about 40 cm^{-1} (boson peak), as well as in the ranges from 60 to 80 cm^{-1} (β-TeO_2) and from 110 to 143 cm^{-1} (γ-TeO_2) were not detected due to the use of a band-reject filter. The broad band with a maximum in the 400 – 500 cm^{-1} range is associated with the stretching and compression of the Te–O–Te bridging bonds in the structural elements of TeO_4, TeO_3, $TeO_{3+\delta}$. Two Raman bands located between 600 and 900 cm^{-1} are related to vibrations in the network of trigonal bipyramids of TeO_4, antisymmetric vibrations of the Te–O–Te chemical bonds and stretching of non-bridging Te–O bonds [17]. When activating glasses with magnetite, a relative increase in the intensity of the band with a maximum at about 420 – 430 cm^{-1} was detected, which indicates the dissolution of iron oxide in the glass, accompanied by the rupture of Te–O–Te bridging bonds. The work [6] showed that the use of corundum crucibles in the process of obtaining glasses leads to alumina dissolution in the glass matrix, causing a significant increase in the Raman scattering signal in the range from 750 to 800 cm^{-1}. The Fe_3O_4, α-Fe_2O_3, γ-Fe_2O_3, and FeO oxides also give a Raman scattering signal in the range from 500 to 800 cm^{-1} [18]. The Raman spectra of crystalline tetragonal $BaTiO_3$ contain bands with maxima at 237 (A_1(TO)), 296 (B_1, E(TO + LO)), 506 (A_1(TO), E(TO)), and 714 cm^{-1} (A_1(LO), E(LO)) [19]. The signals from iron oxides and $BaTiO_3$ intensify the response formed by the glass matrix and partially overlap with this response signal.

Figure 2*b* shows that non-activated zinc–tellurite glass exhibits the highest transparency with an absorption edge of 3.10 eV. Following addition of 1 mol.% barium titanate to the glass, the absorption edge shifts to the ultraviolet spectrum toward the value of 2.90 eV. When 1 mol.% magnetite is introduced into the glass, the absorption edge shifts to the

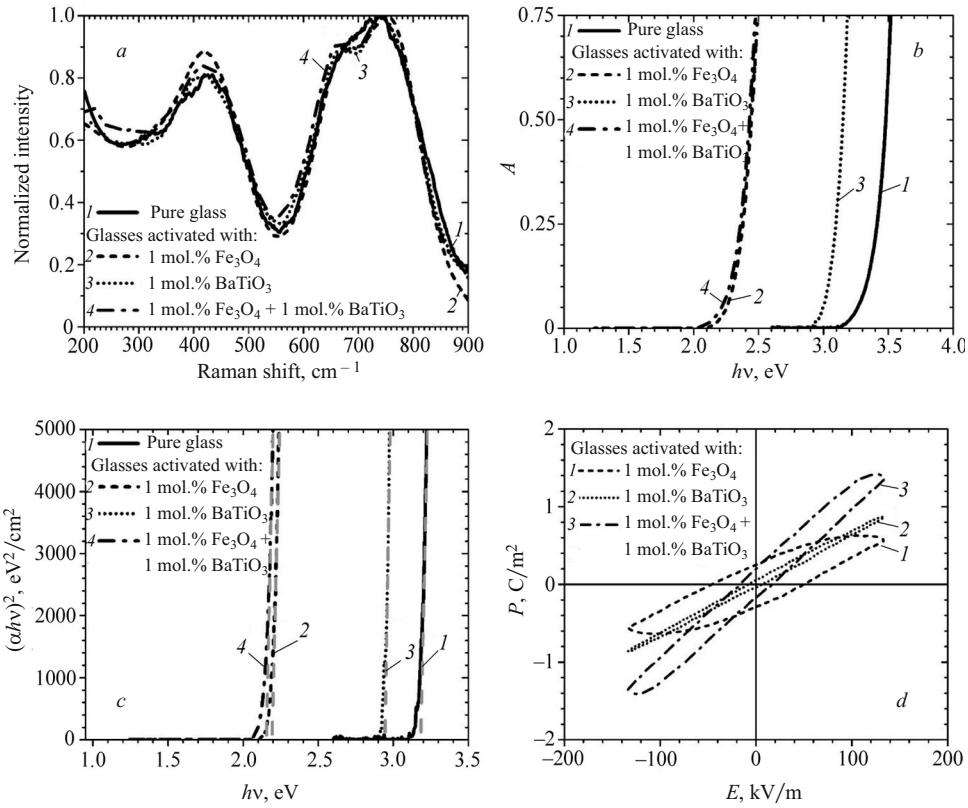

Fig. 2. Raman spectra (*a*) and absorption spectra (*b*) of zinc–tellurite glasses; Davis–Mott plots (*c*) and hysteresis loops of electric polarization (*d*) of samples under an electric field frequency of 1 kHz.

visible spectrum, comprising 2.10 eV. The absorption spectra of the glasses activated simultaneously with 1 mol.% Fe_3O_4 and 1 mol.% $BaTiO_3$ are distinguished by a minor (0.06 eV) shift of the absorption edge toward the low-energy region relative to the previous sample. The absorption spectra exhibit no additional signals, with the exception of the observed shifts in the energy of the absorption edge of the glasses in the UV and visible spectrum.

According to the Davis–Mott theory [20, 21], the dependence of the optical absorption coefficient on the incident photon energy is determined by expression (1), which allows the bandgap value to be calculated:

$$\alpha = \frac{C\left(h\nu - E_g\right)^l}{h\nu}, \qquad (1)$$

where the absorption coefficient $\alpha = \frac{2.303A}{d}$; A is the absorbance magnitude; d is the sample thickness; C is the energy-independent constant; $h\nu$ is the photon energy; E_g is the bandgap; l is the constant determined by the type of optical transitions. The optical absorption spectra of all glasses show only intense edge absorption characteristic of direct transitions, with any bands or peaks indicating the presence of impurity absorption being absent. The data shown in Fig. 2*c* in the form of a graphical Davis–Mott dependence with a coefficient $l = 1/2$ were used to determine the bandgap values of the glasses. The absolute bandgap values of pure glass and glasses activated with barium titanate, magnetite, as well as magnetite and barium titanate in combination, comprised 3.19, 2.94, 2.19, and 2.16 eV, respectively. The obtained data and expression (2) [16] were used to calculate the absolute values of refractive index (n) of the glass samples:

$$\frac{n^2 - 1}{n^2 + 2} = 1 - \sqrt{\frac{E_g}{20}}. \qquad (2)$$

The absolute value of the refractive index of pure glass was 2.35. The refractive indices of glasses activated with barium titanate, magnetite, as well as magnetite and barium titanate in combination, were 2.41, 2.66, and 2.67, respectively. The obtained bandgap and refractive index values were found to agree well with the data of other publications on zinc–tellurite glasses [14, 22]. The dependencies of the electric polarization P of the studied materials on the applied external voltage are shown in Fig. 2*d*. All activated glasses demonstrated a hysteresis of electric polarization in an external electric field at room temperature. Table 1 presents the main parameters of electric hysteresis loops, i.e., the values of the coercive field E_c and residual polarization P_r.

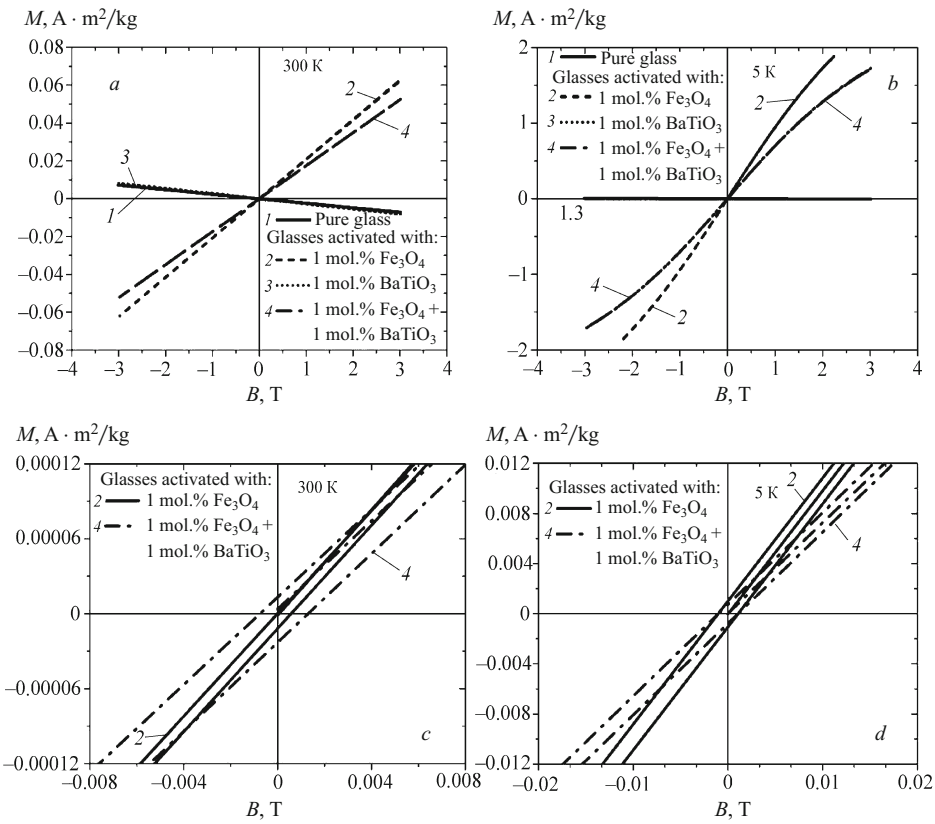

Fig. 3. Results of SQUID magnetometry of nominally pure and activated glasses at temperatures of 300 K (*a*, *c*) and 5 K (*b*, *d*).

The authors of [14] observed an increase in the polarizability and refractive index of zinc–tellurite glasses upon their modification with Fe_3O_4 at a concentration of up to 1 mol.%. This result was explained by the formation of non-bridging oxygen atoms and the stabilization of Fe^{2+} ions in the Fe_3O_4 compound in the glass matrix. In the glasses studied in our work, activation with magnetite nanoparticles produced a similar effect, accompanied by the formation of charged iron oxide clusters. When synthesizing glasses activated with barium titanate nanoparticles, the charge interaction occurring due to the partial decomposition of the activator substance leads to the formation of clusters of nanosized $BaTiO_3$, individual Ba^{2+} ions, and structural elements of TiO_6. The combined activation of glasses with barium titanate and magnetite, which is converted into γ-Fe_2O_3 during synthesis [23], leads to a decrease in the absolute values of their electric polarization, i.e., an effective suppression of the processes related to the formation of charge-ordered (polarized) areas in glasses.

TABLE_1. Characteristics of Electrical Hysteresis Loops of Glasses Activated by Magnetite and Barium Titanate Nanoparticles

Glass composition	E_c, kV/m	P_r, C/m^2
$20ZnO–79TeO_2–1Fe_3O_4$	49.6	0.251
$20ZnO–79TeO_2–1BaTiO_3$	7.1	0.055
$20ZnO–78TeO_2–1Fe_3O_4–1BaTiO_3$	17.2	0.194

Figure 3 shows the dependence of the specific magnetization M of the samples on the applied magnetic field at temperatures of 300 and 5 K. Pure glass and the glass activated only with barium titanate nanoparticles demonstrate linear magnetic-field dependencies characteristic of diamagnets with diamagnetic response values of –0.0024 A · m^2/(kg · T) and –0.0027 A · m^2/(kg · T) at 300 K. The decrease in temperatures to 5 K eliminates the difference in the diamagnetic lines for glasses ($20ZnO – 80TeO_2$ and $20ZnO – 79TeO_2 – 1BaTiO_3$), with the response value in the magnetic field being –0.0012 A · m^2/(kg · T) in both cases.

Activation with magnetite makes the glasses exhibit signs of paramagnetic properties. At 300 K, the paramagnetic response of the magnetite-modified glass equals 0.0208 A · m^2/(kg · T). After activation of the samples with barium titanium nanoparticles, the paramagnetic response decreases to 0.0175 A · m^2/(kg · T). At low (5 K) temperatures, the magnetic field dependencies of the specific magnetization of the samples acquire an *S* shape with open partial hysteresis loops. This indicates the emergence of (ferro-) ferrimagnetic ordering in the glasses. At the same time, an increase in the absolute value of paramagnetic response to values of 0.9290 and 0.6760 A · m^2/(kg · T) is observed in

TABLE 2. Characteristics of Magnetic Hysteresis Loops of Glasses Activated by Magnetite and Barium Titanate

Glass composition	300 K		5 K	
	B_c, T	M_r, A · m^2/kg	B_c, T	M_r, A · m^2/kg
20ZnO–79TeO_2–1Fe_3O_4	0.0006	0.00001	0.0011	0.0010
20ZnO–78TeO_2–1Fe_3O_4–1$BaTiO_3$	0.0013	0.00001	0.0011	0.0007

the glasses activated by magnetite and magnetite plus barium titanate nanoparticles, respectively. Figure 3*c* and *d* (on an enlarged scale) demonstrates open enlarged loops of magnetic hysteresis of the glasses, the characteristics of which are presented in Table 2.

Despite the observed hysteresis loops of electric polarization, the synthesized glasses cannot be considered ferroelectrics. Indeed, these materials do not have a polar symmetry axis and, in the studied range of changes in the external electric field, the hysteresis loops do not reach saturation of the electric polarization value [24, 25]. The authors in [23] made a hypothesis about the formation of magnetic clusters of γ-Fe_2O_3 iron oxide during the synthesis of tellurite glasses activated by magnetite nanoparticles. Our data obtained based on the analysis of changes in the polarization properties of the samples indicate that the electrical response in the glasses may be generated by various charged centers. The activation of glass with magnetite led to the production of weakly magnetic glasses, in which an electrically polarized state is formed when an external electric field is applied. The magnetite-activated glasses demonstrated the strongest electric and magnetic hysteresis. The combined activation of glass with magnetite and barium titanate weakens the magnetic response and electric polarization compared to glasses activated only with magnetite. Thus, the data obtained indirectly confirm the hypothesis about the formation of magnetoactive clusters of γ-Fe_2O_3 iron oxide. The modification of glass with barium titanate nanoparticles practically does not lead to the formation of ferro- and magnetoactive clusters or particles in such glasses; on the contrary, it has a negative effect on the formation of electro- and magnetoactive regions in magnetite-activated zinc–tellurite glasses.

The work was carried out with the financial support of the strategic academic leadership program "Priority 2030" (project No. 075-15-2024-200 of February 6, 2024).

CONCLUSIONS

The melt quenching technique was used to synthesize nominally pure zinc–tellurite glasses (20ZnO – 80TeO_2) and those activated with magnetite (20ZnO – 79TeO_2 – 1Fe_3O_4), barium titanate (20ZnO – 79TeO_2 – 1$BaTiO_3$), as well as by magnetite and barium titanate nanoparticles (20ZnO – 78TeO_2 – 1Fe_3O_4 – 1$BaTiO_3$) in combination. The study of their optical properties confirmed the decrease in the bandgap value from 3.19 eV in undoped glass to 2.16 – 2.94 eV depending on the type of the activator particles. Upon activation of the glasses, spin-charge ordered regions appear, which produce electric and magnetic responses to external electric and magnetic fields. The data obtained on the polarization and magnetic properties of the samples render zinc–tellurite glasses activated by nanosized particles of magnetite and barium titanate to be promising for obtaining multiferroic materials, in which the coexistence of interacting electrical and magnetic ordering is possible.

REFERENCES

1. J. Majzlan, S. Notz, P. Haase, et al., "Thermodynamic properties of tellurite (β-TeO_2), paratellurite (α-TeO_2), TeO_2 glass, and Te (IV) phases with stoichiometry $M_2Te_3O_8$, MTe_6O_{13}, MTe_2O_5 (M^{2+} = Co, Cu, Mg, Mn, Ni, Zn)," *Geochemistry*, **82**, 125915 (2022).
2. A. Novatski, A. Somer, A. Gonçalves, et al., "Thermal and optical properties of lithium-zinc-tellurite glasses," *Mater. Chem. Phys.*, **231**, 150 – 158 (2019).
3. J. de Clermont-Gallerande, D. Taniguchi, M. Colas, et al., "Influence of Nd^{3+} modifying on 80TeO_{2-x}ZnO – (20 – x)Na_2O ternary glass system," *APL Mater.*, **9**, 111111 (2021).
4. J. de Clermont-Gallerande, M. Dutreilh-Colas, F. Célarié, et al., "Correlation between mechanical and structural properties as a function of temperature within the TeO_2–TeO_2–ZnO ternary system," *J. Non-Cryst. Solids*, **528**, 119716 (2020).
5. E. Stavrou, C. Tsiantos, R. D. Tsopouridou, et al., "Raman scattering boson peak and differential scanning calorimetry studies of the glass transition in tellurium–zinc oxide glasses," *J. Phys. Condens. Matter.*, **22**, 195103 (2010).
6. N. S. Tagiara, D. Palles, E. D. Simandiras, et al., "Synthesis, thermal and structural properties of pure TeO_2 glass and zinc–tellurite glasses," *J. Non-Cryst. Solids*, **457**, 116 – 125 (2017).
7. O. A. Zamyatin, M. F. Churbanov, J. A. Medvedeva, et al., "Glass-forming region and optical properties of the TeO_2–ZnO–NiO system," *J. Non-Cryst. Solids*, **479**, 29 – 41 (2018).
8. O. A. Zamyatin, O. A. Lomteva, and M. F. Churbanov, "Specific absorption coefficient of cobalt (II) ions in molybdenum-containing tellurite–zinc glass," *Neorganicheskie Materialy*, **57**, 306 – 312 (2021).
9. O. A. Zamyatin, M. F. Churbanov, and E. V. Zamyatina, "Specific absorption coefficient of Cr^{3+} ions in $(TeO_2)_{0.70}(ZnO)_{0.30}$ glass," *Neorganicheskie Materialy*, **55**, 750 – 755 (2019).
10. E. A. Anashkina, V. V. Dorofeev, S. V. Muravyov, et al., "Possibilities of laser amplification and measurement of the field structure of ultrashort pulses in the range of 2.7 – 3 μm in erbium-doped tellurite glass fiber light guides," *Kvantovaya Elektronika*, **48**, 1118 – 1127 (2018).
11. S. H. Alazoumi, S. A. Aziz, R. El-Mallawany, et al., "Optical properties of zinc lead tellurite glasses," *Results Phys.*, **9**, 1371 – 1376 (2018).

12. F. A. Ali, N. S. Sabri, and M. K. Talari, "Effect of ZnO–TeO_2 glass doping on structural and dielectric properties of $BiFeO_3$ prepared by solid state method," *Solid State Sci. Technol*., **24**, 93 – 100 (2016).
13. W. Widanarto, M. R. Sahar, S. K. Ghoshal, et al., "Thermal, structural and magnetic properties of zinc-tellurite glasses containing natural ferrite oxide," *Mater. Lett*., **108**, 289 – 292 (2013).
14. W. Widanarto, M. R. Sahar, S. K. Ghoshal, et al., "Natural Fe_3O_4 nanoparticles embedded zinc–tellurite glasses: polarizability and optical properties," *Mater. Chem. Phys*., **138**, 174 – 178 (2013).
15. M. V. Shestakov, X. Chen, W. Baekelant, et al., "Lead silicate glass SiO_2–PbF_2 doped with luminescent Ag nanoclusters of a fixed site," *RSC Adv.*, **4**, 20699 – 20703 (2014).
16. V. D. Rodríguez, V. K. Tikhomirov, J. J. Velázquez, et al., "Visible-to-UV/violet upconversion dynamics in Er^{3+}-doped oxyfluoride nanoscale glass ceramics," *Adv. Opt. Mater.*, **1**, 747 – 752 (2013).
17. A. K. Yadav and P. Singh, "A review of structure of oxide glasses by Raman spectroscopy," *RSC Adv.*, **5**, 67583 – 67609 (2015).
18. M. Testa-Anta, M. A. Ramos-Docampo, M. Comesaña-Hermo, et al., "Raman spectroscopy to unravel the magnetic properties of iron oxide nanocrystals for bio-related applications," *Nanoscale Adv.*, **1**, 2086 – 2103 (2019).
19. V. S. Vinita, G. G. S. Rao, J. Samuel, et al., "Structural, Raman and optical investigations of barium titanate nanoparticles," *Phosphorus Sulfur Silicon Relat. Elem.*, **197**, 169 – 175 (2022).
20. W. Widanarto, M. R. Sahar, S. K. Ghoshal, et al., "Effect of natural Fe_3O_4 nanoparticles on structural and optical properties of Er^{3+} doped tellurite glass," *J. Magn. Magn. Mater.*, **326**, 123 – 128 (2013).
21. A. A. A. Awshah, U. S. Aliyu, H. M. Kamari, et al., "Polarizability and optical properties of TeO_2–ZnO glass system doped with Nd_2O_3," *J. Mater. Sci. Mater. Electron*., **33**, 13493 – 13505 (2022).
22. R. Stefan, M. Karabulut, A. Popa, et al., "A spectroscopic study of the influence of ÑuO addition on the ZnO–TeO_2 glass and glass ceramics," *J. Non-Cryst. Solids*., **498**, 430 – 436 (2018).
23. M. V. Shestakov, I. I. Makoed, and V. V. Moshchalkov, "Synthesis and magnetic properties of zinc-tellurite glasses activated by magnetite nanoparticles," *Fiz. Tverd. Tela*, **65**, 803 – 809 (2023).
24. R. K. Vasudevan, N. Balke, P. Maksymovych, et al., "Ferroelectric or non-ferroelectric: why so many materials exhibit "ferroelectricity" on the nanoscale," *Appl. Phys. Rev.*, **4**, 021302 (2017).
25. Z. Tylczyński, "A collection of 505 papers on false or unconfirmed ferroelectric properties in single crystals, ceramics and polymers," *Front. Phys.*, **14**, 63301 (2019).